# Old Dark Energy

Marina Cortês[1] and Eric V. Linder[1,2,3]
[1]*Berkeley Lab, Berkeley, CA 94720, USA*
[2]*University of California, Berkeley, CA 94720, USA and*
[3]*Institute for the Early Universe, Ewha Womans University, Seoul, South Korea*
(Dated: March 15, 2010)

Dark energy dynamics in the recent universe is influenced by its evolution through the long, matter dominated expansion history. A particular dynamical property, the flow variable, remains constant in several classes of scalar field models as long as matter dominates; the dark energy is only free to diverge in behavior at recent times. This gives natural initial conditions for Monte Carlo studies of dark energy dynamics. We propose a parametrization for the later evolution that covers a wide range of possible behaviors, is tractable in making predictions, and can be constrained by observations. We compare the approach to directly parametrizing the potential, which does not take into account the maturity of the dark energy dynamics.



## I. INTRODUCTION

Very little is known about the dynamics of dark energy, other than that at redshifts $z \gtrsim 1$ the expansion history gives way to a matter dominated era. However, this fact is powerful in narrowing the possible behaviors of dark energy because the matter-dominated Hubble friction plays a major role in the dark energy dynamics. That is, the dark energy field $\phi$ evolves for a long time in a particular environment – by the time dark energy comes to contribute significantly to the expansion it is an old, or "mature", field.

The influence of matter domination on the dark energy dynamics is very different than the slow-roll conditions for an inflationary field in the early universe. Dark energy does not satisfy slow-roll conditions on the potential $V$ for most of its evolution, unless it is highly fine tuned [1]. Instead, the matter domination can create a definite relation between the deviation of the dark energy density $\Omega_\phi$ from 0, the deviation of its equation of state $w$ from $-1$, and the characteristic scale of the potential, $(1/V)dV/d\phi$ (which is sometimes called the first slow-roll parameter, but here does not need to be small). A particular combination of them is called the flow parameter by [2] and is essentially constant during matter domination.

In this paper we examine the dark energy evolution after matter domination wanes, by parametrizing the deviation of the flow parameter from its constant value during matter domination. Since the constancy holds up until quite late redshifts, $z \approx 2$, the dark energy has a restricted ability to exhibit diverse dynamics by the present. This allows the three parameter flow form we present to reasonably approximate a wide range of the possible behaviors.

Any form containing few parameters will not in general be able to describe every possible behavior so interesting questions include whether it captures key physics, reasonably describes the major classes of behavior, and can be constrained by observations. In particular, the dynamics should include the thawing and freezing classes [3], which respectively depart from and approach cosmological constant behavior within specific regions of the $w$-$w'$ phase space. But it should also be flexible enough to permit models outside these regions and have the physics and data determine which are viable.

In §II we discuss the implications of a long matter dominated era in guiding the dark energy dynamics and the role of the flow parameter. We present our approach to evolution as dark energy increases in importance in §III and study the resulting behaviors. Constraints on the $w$-$w'$ and flow parameters phase spaces from future observations are investigated in §IV. We compare the flow approach to parametrizing the potential in §V, discussing the different weights these impose on the dynamics and the thawing vs. freezing classes.

## II. MATURE DYNAMICS

During the early universe accelerated expansion of inflation, the inflaton scalar field dominates the total energy density and so the field evolution is essentially wholly determined by its potential. Once inflation ends, the cosmic expansion is dominated by radiation and then matter. The expansion rate – the Hubble parameter $H$ – is rapid and the Hubble drag influences the evolution of any light scalar field that may eventually cause a more recent universe acceleration.

The evolution of this scalar field is determined by the Klein-Gordon equation

$$\ddot\phi + 3H(\rho_b, \rho_\phi)\,\dot\phi + V_\phi = 0\,, \tag{1}$$

where we have explicitly indicated the dependence of the Hubble parameter on the background energy density $\rho_b$ and the scalar field density $\rho_\phi$. The energy density $\rho_\phi = V(\phi) + (1/2)\dot\phi^2$, the sum of the potential and kinetic energies, so we cannot determine the field evolution without knowing $V(\phi)$ and the initial conditions $\phi_i$ and $\dot\phi_i$. Formally, then, we cannot say anything completely general about the dark energy dynamics.

However, an initial kinetic energy much larger than the potential, $K \gg V$, will rapidly redshift away, $\dot\phi \sim a^{-3}$ as can be seen by neglecting the last term in Eq. (1). So we

expect the kinetic energy of the field does not dominate, but rather the background fluid (radiation or matter) does. See [4–6] for early papers on cosmological scalar fields, or quintessence. The distance $\Delta\phi$ the field rolls can be estimated by approximating $\dot\phi \approx \Delta\phi/\Delta t$ and using $K = (1/2)\rho_\phi\,(1+w)$, where the equation of state $w = [(K/V)-1)]/[(K/V)+1]$. Then

$$\Delta\phi \sim \sqrt{(1+w)\,\rho_\phi\,(\Delta t)^2}\,. \tag{2}$$

If the Hubble friction is large, then the characteristic timescale of the field evolution may be the Hubble time $H^{-1}$, so the square root contains $\rho_\phi/H^2 \sim \Omega_\phi$ which is small in the matter (or radiation) dominated era. So the era of background domination has significant effect on the dark energy dynamics.

If the potential dominates the kinetic energy then $1+w$ is very small as well and so both factors lead to $\Delta\phi \ll 1$ during the background domination (although by today, with dark energy domination, the condition $\Delta\phi \ll 1$ generally does not hold; see Sec. V). This class is known as thawing fields. In other cases $1+w$ does not start small and the field can roll further.

If the potential has particular forms, the field can possess an attractor trajectory (see, e.g., [4, 5, 7–10]). In this case the equation of state is determined by the background component and the parameters of the potential, independent of initial conditions. The potential and kinetic energies are locked in a set ratio such that the equation of state is constant during background domination; the fields are then known as trackers.

In any case, the dark energy density is not exactly zero and the equation of state is not exactly $-1$. It is interesting to consider how these deviations are related to each other in the background dominated era. Ref. [2] showed (also see [11]) that one could define a combination of these deviations, together with the characteristic scale of the potential, that held constant during the long matter dominated expansion. Ref. [2] defined

$$F \equiv \frac{1+w}{\Omega_\phi \lambda^2}\,, \tag{3}$$

where $1+w$ is the equation of state deviation, $\Omega_\phi$ the dark energy density in units of the critical density, and $\lambda = -(1/V)dV/d\phi$ gives a characteristic field scale. Despite all these quantities varying as the universe expands and the field evolves, the flow combination $F$ remains almost constant.

Written in terms of the dark energy dynamics,

$$w' = -3(1-w^2)\left[1 - \frac{1}{\sqrt{3F}}\right]\,, \tag{4}$$

where $w' = dw/d\ln a$. Thus the long matter dominated era, which imposes $F =$ constant until quite late times, $z \approx 2$, (except for specifically fine tuned fields) effectively imposes constraints on the dark energy dynamics. That is, the dark energy is an old field that lived for many $e$-folds of expansion in a matter dominated environment. Choosing an arbitrary dynamics amounts to either ignoring this physical influence or embracing a fine tuning of the field's initial conditions.

A direct parametrization of the potential (see, e.g., [12–16]), and Monte Carlo variation of its parameters à la the interesting dynamics work of [15, 17], will not in general take into account the maturity. While one could parametrize the equation of state in such a way as to incorporate the appropriate condition (see, e.g., [1, 3, 11, 18]), we choose to study the flow parameter since it possesses the interesting properties of being nearly constant during matter domination and incorporating $\Omega_\phi$, the natural quantity for measuring the deviation from matter domination as it begins to break.

## III. EVOLVING DYNAMICS

During matter domination, fields which slowly relax from being frozen by the high Hubble friction – thawing fields – possess $F = 4/27$ [2]. Equivalently, they thaw from the cosmological constant state along the trajectory $w' = 3(1+w)$ according to Eq. (4). Tracker fields possess $F = 1/3$ or $w' = 0$. Fields with other behaviors are certainly possible, but these behaviors will be sensitive to the specific initial conditions. However in this section we will briefly consider other high redshift values for $F$.

We are most interested in how the dark energy evolves as matter domination wanes, and as eventually dark energy comes to dominate by the present. That is, we want to extend the asymptotic, matter dominated behavior to greater dynamical freedom in the present. Calculating the first order (in the dark energy density fraction) corrections to the dynamics [2] gives a flow parameter behavior

$$F \approx F_0 + \beta\, a^B\,, \tag{5}$$

where $F_0$ is the matter dominated constant value, $\beta$ is related to the dark energy density $\Omega_\phi$, and $B = 3$ (or $-3w_\infty$ where $w(z \gg 1) = w_\infty$ in the thawing (or tracking) case.

However, since today the ratio of dark energy density to matter density is nearly 3, we do not expect the first order solution to be valid. Numerical solutions, for example, show that $F$ can grow by factors of order two to three. Therefore, although we will keep the form (5) we take $\beta$ and $B$ to be free parameters representing effective fits over the expansion history between high redshift matter domination and today.

The form (5) has the advantage that, upon substitution into Eq. (4), one can analytically solve for the dynamics

$w(a)$. The result is

$$w = \frac{\chi-1}{\chi+1}, \quad (6)$$

$$\chi = \frac{1+w_i}{1-w_i}\left(\frac{a}{a_i}\right)^{-6} \quad (7)$$

$$\times\left[\frac{\sqrt{F}-\sqrt{F_0}}{\sqrt{F}+\sqrt{F_0}}\frac{\sqrt{F_i}+\sqrt{F_0}}{\sqrt{F_i}-\sqrt{F_0}}\right]^{6/(B\sqrt{3F_0})}, \quad (8)$$

where $F_i = F(a_i)$, $w_i = w(a_i)$, and $a_i$ is some initial scale factor, e.g. in the matter dominated regime. The four parameters are therefore $F_0$, $\beta$, $B$, and $w_i$, and we choose $a_i = 0.1$ (the exact value of $a_i$ is unimportant as long as it is well within the matter dominated era).

As the flow $F$ increases as the dark energy density becomes more important, the field evolves further in the direction of the skating curve, $w' = -3(1-w^2)$, where the potential slope is unimportant and field moves – skates [14, 19] – with a rapidly redshifting kinetic energy. For thawing fields, this means that the dynamics can actually turn around and head back toward the frozen, cosmological constant state. Recall that thawing fields start with $F_0 = 4/27$, so their maximum, turnaround value of $w$ occurs when $F$ has risen to $1/3$, at which point $w' = 0$. For freezing fields, the increase in $F$ simply moves them faster toward the cosmological constant.

Figure 1–2 show the effects of each parameter on the dynamics, for the thawing and freezing cases. The amplitude parameter $\beta$ controls the degree of evolution from the matter dominated state – increasing $\beta$ has the same effect as increasing $F$. The transition parameter $B$ governs the rapidity of evolution – larger $B$ means that the transition from the matter dominated behavior happens nearer to the present.

The initial condition parameters $F_0$ and $w_i$ have a significant influence, as seen in Fig. 3. Increasing $F_0$ gives the dynamics a significant push in its evolution. If $F_0 \neq 4/27$ then the field somehow ignores the high Hubble friction during matter domination. Basically the field must have been "super-accelerating", i.e. $\ddot\phi \gg H\dot\phi$, if $F_0 < 4/27$, while it must have been fine tuned to be coasting $\ddot\phi \ll H\dot\phi$ (not slow-roll since the matter, not the dark energy, dominates the expansion) if $4/27 < F_0 < 1/3$ (cf. [1]). The value $F_0 = 1/3$ corresponds to the dynamics determined by an attractor solution for the field, but $F_0 > 1/3$ indicates "super-deceleration", $-\ddot\phi \gg dV/d\phi$, equivalent to fine tuning for a "super-flat" potential, yet somehow the field still rolls. These properties motivate why we will later consider only the values $F_0 = 4/27$ and $1/3$.

Similarly, increasing $w_i$ for thawing fields gives a strong boost to the evolution, pushing the dynamics far from $w = -1$. (For tracker freezer fields, $w_i$ is determined by the attractor solution and then $w_i' = 0$.) For thawing fields, we expect $1 + w_i$ to be of order $\Omega_{\phi,i}$, the dark energy density at the initial redshift considered in the matter dominated era (see, for example, [2]). (Taking $a_i = 0.1$, typically $w_i \approx -1+10^{-4}$.) For freezing fields $w_i$ can be of order unity, but again tracking evolution starts

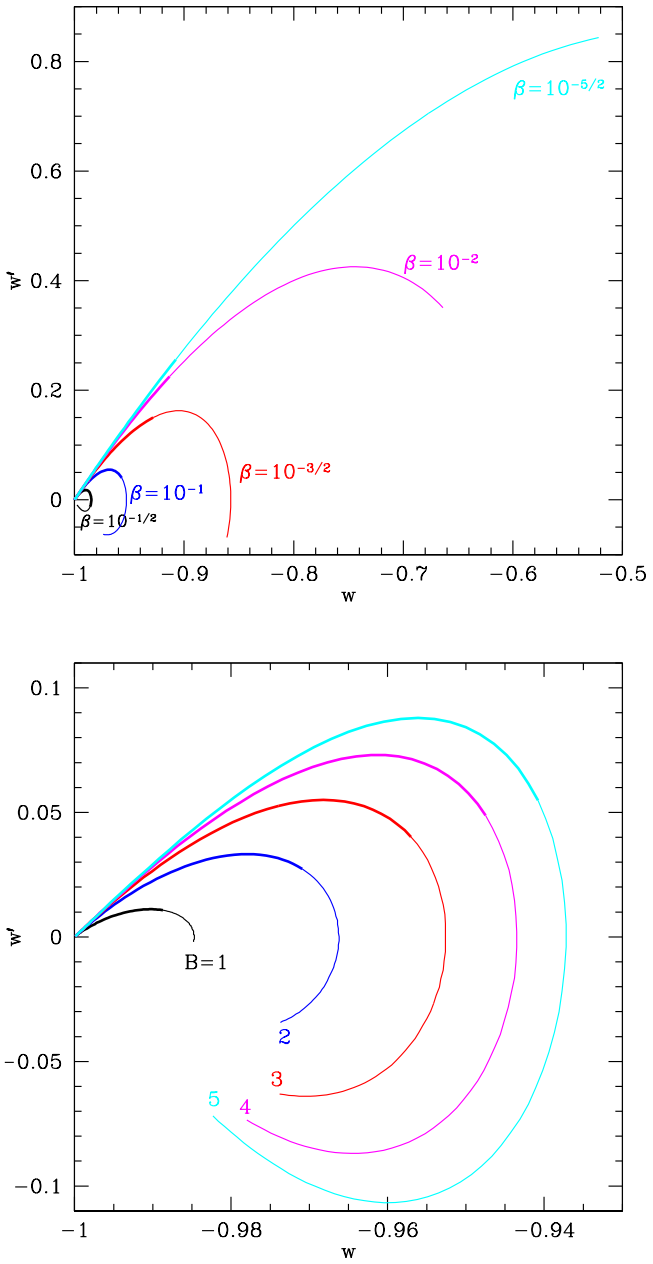


FIG. 1: [Top panel] The deviation amplitude of the flow parameter between the matter dominated era and today is given by $\beta$. Increasing $\beta$ moves the dynamics away from small field deviations and toward skating, with rapid approach toward a frozen state. [Bottom panel] For a fixed deviation amplitude, the transition rapidity is determined by $B$. Increasing $B$ postpones the transition from the matter dominated flow parameter, causing a more rapid evolution close to the present. Both panels are for the thawing case, with $F_0 = 4/27$, and $1 + w_i = 10^{-4}$; curves extend to $a = 2$ with thick portions of curves for $a \leq 1$.

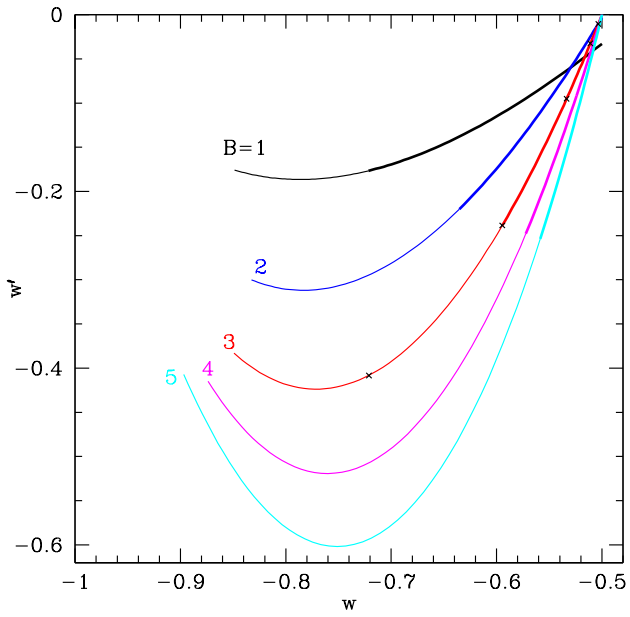


FIG. 2: As the bottom panel of Fig. 1 but for the freezing case, with $F_0 = 1/3$, and $w_i = -0.5$. Variation of $\beta$, as in Fig. 1 top panel, tends to move the evolution along the curves; for example for $B = 3$ we show by x's the $a = 1$ location for $\beta = 10^{-5/2}$, $10^{-2}$, $10^{-3/2}$, $10^{-1}$, $10^{-1/2}$, from right to left.

with $w' = 0$. Another aspect of non-standard values of $F_0$ or $w_i$ is the presence of excessive early dark energy density. For example, a thawing field with $1 + w_i = 10^{-2}$ has $\Omega_{\phi,i} \approx 0.06$, which would cause conflict with growth of large scale structure and the cosmic microwave background observations [20]. A thawing field with $F_0 = 1.5/27$ would break matter domination completely.

Thus, we effectively have a three parameter description, given by the set $\{\beta, B, w_i\}$, for each of two cases: $F_0 = 4/27$, $1/3$. In general even a three parameter description of dark energy dynamics cannot be fully constrained even with next generation data [21, 22]. Indeed, determining the transition time or speed for the dark energy equation of state is extremely difficult [21, 23, 24] so we do not expect $B$ to be constrained. However, this form is useful because it gives considerable freedom for dynamics while at the same time taking into account the oldness of dark energy, i.e. the long influence of matter domination on the evolution.

The ansatz also provides for three classes of dynamical behavior: the usual thawing and freezing classes, and "re-freezing" models where the field thaws from the Hubble friction-induced torpor, evolves to a maximum $w$, but then can enter the freezing region and eventually evolve to a potential minimum and cosmological constant state. This last class will be especially interesting as it bounds the area of the $w$-$w'$ plane that lies within a certain observational distance of $\Lambda$, i.e. models that agree with the $\Lambda$CDM expansion history to within a certain precision

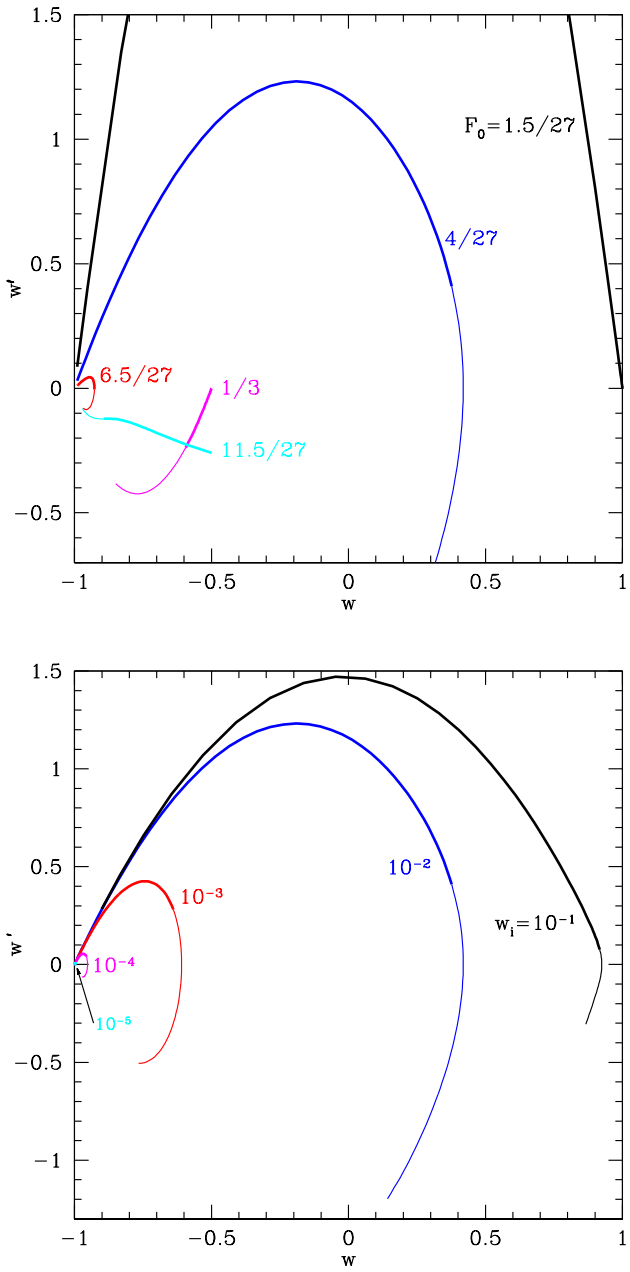


FIG. 3: [Top panel] The flow parameter during matter domination is generally determined to be $F_0 = 4/27$ or $1/3$, but other values are possible with fine tuning. Non-standard values can cause unusual, strong dynamical behavior. For $F_0 \le 6.5/27$ we show curves taking $w_i = -0.99$; larger values of $F_0$ give unobservably small loops. For $F_0 \ge 1/3$ we take $w_i = -0.5$. [Bottom panel] The dark energy equation of state at some fixed redshift in the matter dominated era can give a strong thrust to the evolution for thawing models if it is not near the thawing value $w_i = -1$ expected from Hubble drag.

(see the next section). One can imagine a fourth class which starts as trackers but then turns away from the cosmological constant, i.e. somehow moves away from the

minimum, but there is little physical motivation for this and we do not consider it further.

## IV. CONSTRAINING DYNAMICS

In the previous section we saw that rich dynamics is still available to the dark energy field, even after taking into account its oldness – the effect of the long era of matter domination to age and mellow the arbitrariness of the early evolution. In particular, we emphasized the naturalness of the age influence and did not impose any restrictions on behavior such as assuming small field excursions all the way until late times. Here we consider how observational data will be able to constrain the later time behavior within the flow parameter formulation and narrow in on regions of the $w$-$w'$ plane.

### A. Scanning Phase Space

In fact, we will find clear, bounded regions of the phase space and maximum allowed deviations in $1+w$, assuming some future distance data. To scan over all the possible dynamics within the flow ansatz we begin by considering the parameter ranges. As discussed in the previous section, there are good reasons from both theory and observations to consider *initially* thawing and tracker/freezer classes, with $F_0 = 4/27$ and $1/3$ respectively. We emphasize that these values only give the initial conditions deep in the matter dominated era and are not assuming later behavior.

For $1+w_i$, we indicated that for thawing models this was often around $10^{-4}$, while for freezing models it could lie between a small value and 1, though it is more difficult to achieve $w \approx -1$ today if $w_i$ is not sufficiently negative. However, to keep open all possibilities, we consider $1+w_i$ ranging between $10^{-5}$ and 1, with a log prior for the thawing class. For the amplitude $\beta$, most models generally considered have values between few$\times 10^{-2}$ and few$\times 10^{-1}$. Again to be flexible, we take a log prior between $10^{-5/2}$ and 1. The evolution rapidity $B$ can be examined from the first order correction (in the small dark energy density) to matter domination; for thawing models $B = 3$ and for tracking models $B = -3w_i$. Numerical solutions show that for many thawers $B$ slowly declines toward the present, reaching $\sim 1.5$, and for trackers $B$ slowly rises toward the present, reaching $\sim 2$. We take a generous linear prior on $B$ between 1 and 5.

The models obtained by scanning over the parameter space on a $50\times50\times50$ grid in $\beta$-$B$-$w_i$, for $F_0 = 4/27$ and $1/3$, are then compared in the distance-redshift relation to the distances to redshifts $z = 0.1,\ 0.2,\ldots 1.7$ taking a $\Lambda$CDM fiducial cosmology. The 250,000 generated models are referred to as the prior sample, and those that pass observational cuts are referred to as the viable sample. The observational cut considered first is simply requiring the distances at each redshift to lie within 1% of fiducial (roughly next generation data precision), and the dark energy density at $a_i = 0.1$ must obey $\Omega_{\phi,i} < 0.03$. We later consider a more sophisticated Monte Carlo likelihood calculation.

Figure 4 shows the dynamics in terms of the evolution of the equation of state with scale factor, $w(a)$, for the prior and viable models. While the observations certainly constrain the viable models to more limited *values* of the equation of state, the variety of dynamics allowed by the flow parametrization is still diverse. In particular, models with thawing (leaving $w = -1$), freezing (approaching $-1$), and refreezing (nonmonotonic in $w$) behavior are all represented.

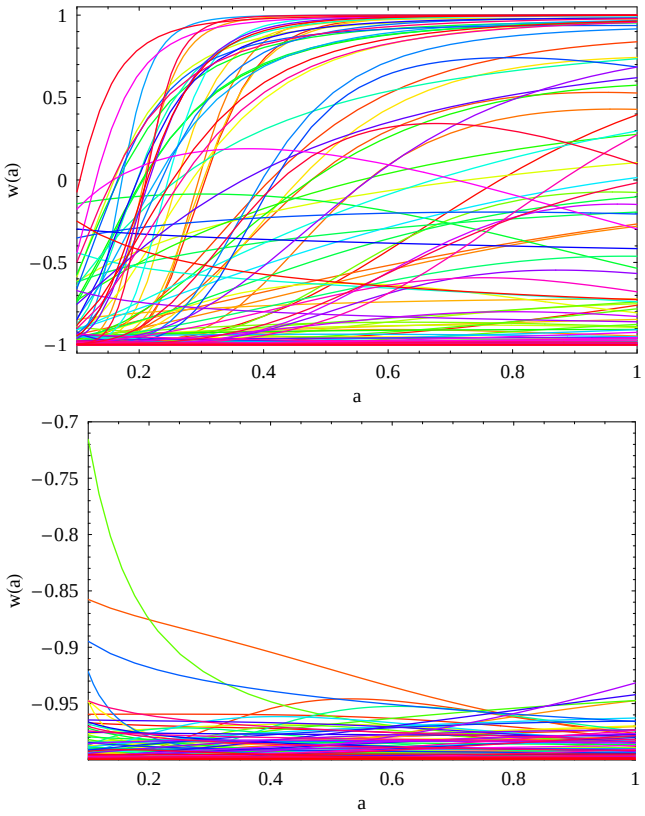


FIG. 4: The flow ansatz allows a rich variety of evolutionary behavior, including nonmonotonicity, while incorporating the physical influence of the long matter dominated era. The top panel shows a random selection of 150 models (note many are very close to $w = -1$) while the bottom panel shows 150 random models that pass the observational cuts. (Note the different vertical scales.) Thawing, freezing, and nonmonotonic evolution are all represented.

Observational constraints translate to well defined regions in the $w$-$w'$ phase space, with a maximum allowed distance deviation imposing a maximum allowed equation of state deviation $w_{\rm max}$. Furthermore, the allowed region is compact, limiting $w'$ as well. Figures 5-6 shows the regions that have less than 1% distance deviation from the $\Lambda$CDM fiducial, with the colors/shading representing different values of $w_i$, as well as scanning over

$\beta$ and $B$. Note that in Fig. 5 for small $1 + w_i$ most models look like regular thawing models, while as $1 + w_i$ increases, the only way the models can obey the observational constraints are to loop around as refreezing models.

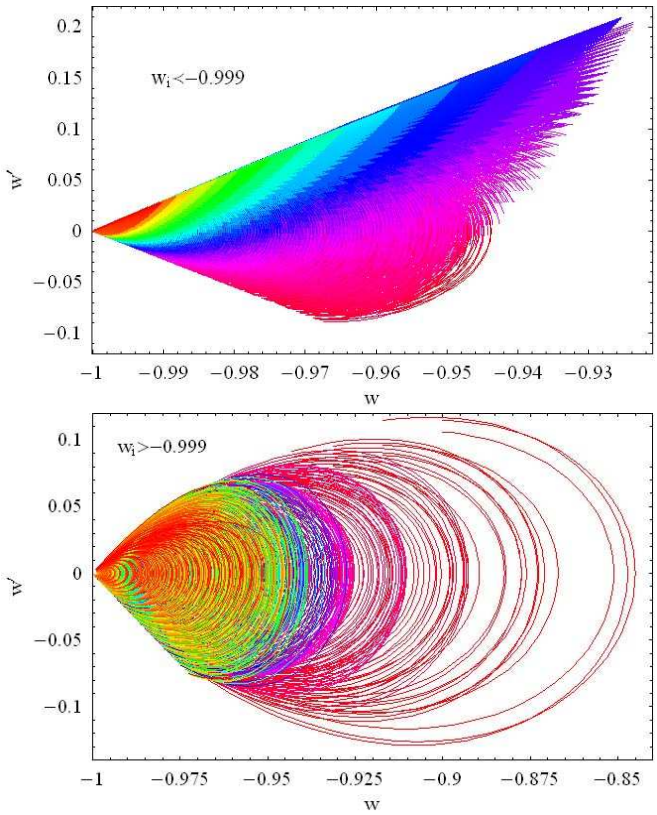


FIG. 5: Models deviating from ΛCDM distances by less than 1% live in a well defined region of phase space, here shown for the initially thawing class. Colors/shading represent different values of $w_i$, with models possessing the smallest values of $1+w_i$ restricted to the bright, red region closest to $w = -1$. The top panel shows models with $w_i < -0.999$ (as expected for most thawing models); the bottom panel shows models with $w_i > -0.999$. The sparseness of the bottom panel is due to the finite gridding: only a tiny percentage of the 2500 models for each $w_i$ pass the distance criteria. The maximum equation of state deviation allowed at any redshift corresponds to $w_{\rm max} = -0.845$.

### B. Mirage Model Dynamics

An interesting special case to consider is those models that deviate from ΛCDM by exactly 1%, rather than those in the whole range 0-1%. These could represent, for example, a specific fiducial distinguishable from ΛCDM by next generation data. Figures 7-8 show the $w(a)$ evolutionary behaviors. Of particular note is the waist near $a = 0.8$, where the equation of state has a dispersion of only $\Delta w \approx 0.01$.

This sort of waist feature has been discussed before in the context of mirage models [25] and pivot points, albeit

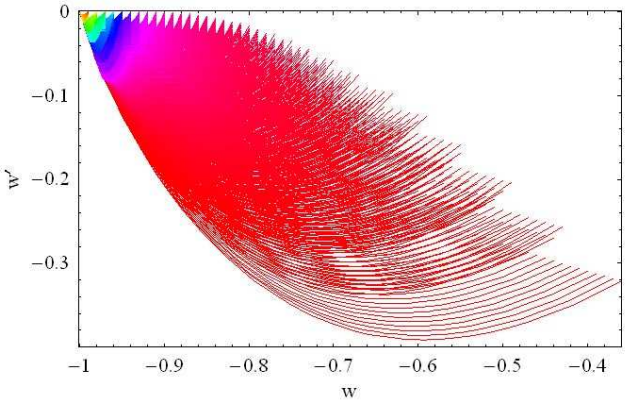


FIG. 6: As Fig. 5, but for the initially freezing class. The maximum initial equation of state deviation, at $a_i = 0.1$, corresponds to $w_{\rm max} = -0.36$, reaching $w_0 = -0.985$ today.

restricted to the parametrization $w(a) = w_0 + w_a(1 - a)$. Such a characteristic highlights the importance of experiments capable of measuring the time variation $w'$ of the equation of state; a survey only able to measure a coarse time average will ineluctably find $\langle w \rangle \approx 0.95$ for all these diverse models. If the dynamical model allowed the equation of state to become more negative than $-1$, then one could easily obtain a waist with ∼0% distance deviation from ΛCDM and find $\langle w \rangle = -1$, wrongly deducing a cosmological constant as the answer. This is the mirage aspect of the mirage models, and so uncovering the true physics behind dark energy requires an experiment with a long redshift baseline over which to measure the time variation of the equation of state.

### C. Dynamics Today

We can also consider the properties of the dark energy today. For initially thawing models, the values of $w_0$ and $w_0'$ can lie basically anywhere within the overall observationally allowed region, e.g. the top panel of Fig. 5 (for the bottom panel, where $w_i > -0.999$, the values today lie at the end of the loops, within the top panel region). For initially freezing models, the distribution today is more interesting. For $w_i$ near $-1$, the values today fill most of the appropriate part of the freezing region in Fig. 6. The region allowed by 1% distance observations is largest when $w_i \approx -0.95$. As $w_i$ increases, however, the dynamics today hugs the lower boundary of the freezing region, $w' = 3w(1+w)$, and the allowed region shrinks, vanishing for $w_i > -0.36$. Figure 9 illustrates these characteristics.

To understand the elements of the dynamics, we show in Fig. 10 the role of the parameters $\beta$ and $B$ on the present value of the equation of state and its time variation, holding $w_i$ fixed. As expected, $\beta$ is more influential than $B$, with large values of $\beta$ accelerating the evolution toward a present state near the cosmological constant.

The original classification of the boundaries of the

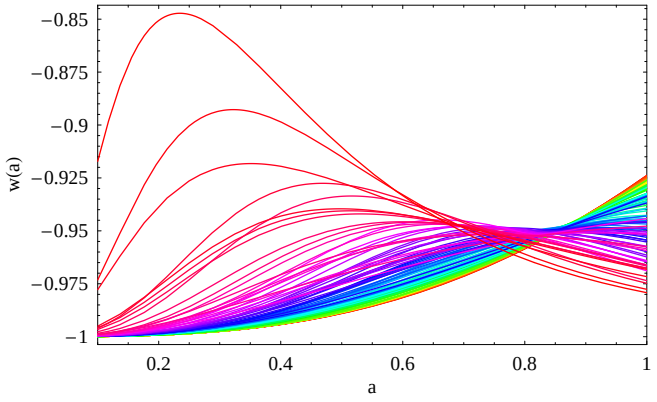


FIG. 7: Initially thawing models that have maximum distance deviations from ΛCDM by some fixed amount, here 0.999–1%, have a variety of behaviors but exhibit a narrow waist at $a \approx 0.8$. In terms of a constant or averaged equation of state, these will all look like $\langle w \rangle \approx -0.95$ but have distinct physics.

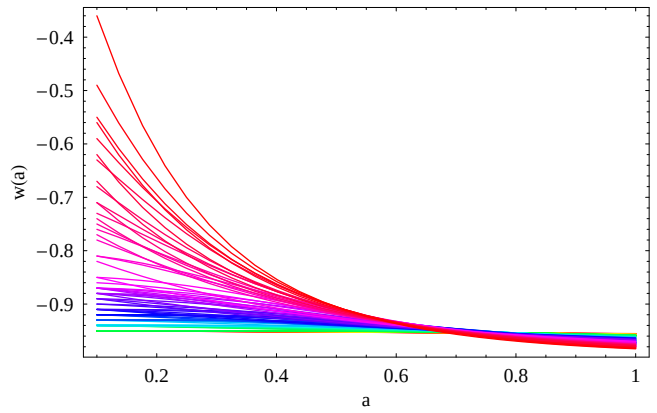


FIG. 8: As Fig. 7 but for freezing models. Note the waist persists, though here it is at $a \approx 0.7$.

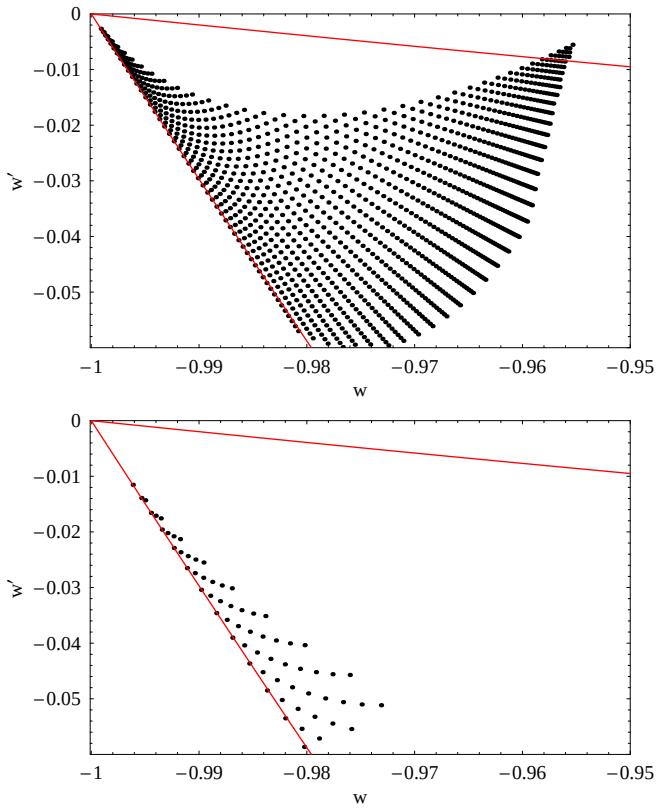


FIG. 9: The dynamics today, $w_0$-$w_0'$, are shown with each dot representing the present endpoint of a trajectory in Fig. 6 for freezing models giving distance deviations of 0–1% from ΛCDM. As $w_i$ moves away from $-1$, the region gradually grows, reaching a maximum extent at $w_i \approx -0.95$ (top panel), then shrinking and coalescing along the bottom boundary of the freezing region (delimited by the straight lines). The bottom panel shows the case of $w_i = -0.8$.

thawing and freezing regions [3] was made by studying numerical solutions for a range of field potentials and determining their endpoints, i.e. $w_0$-$w_0'$ values today. Although the long period of matter domination guides the flow approach dark energy models toward an initial behavior either along the upper boundary of the thawing region, $w' = 3(1+w)$, or to the tracker condition of $w' = 0$ and subsequent approach toward the cosmological constant, we can now address quantitatively whether their evolution leads to consistency with the thawing and freezing regions today.

We clearly see from Fig. 6 that the initially freezing models lie through most of their evolution in the canonical freezing region $0.2w(1+w) \le w' \le 3w(1+w)$, and from Fig. 9 that in particular they all lie in the freezing region today. Recall though that thawing models in the flow approach can either remain thawing, loop around, or even refreeze. Out of all the viable (0-1% distance deviation) initially thawing models, 47% remain in the thawing region through the present, while 40% today lie in what would usually be the freezing region, and 13% today lie between the thawing and region regions near the coasting ($\ddot{\phi} = 0$) line. If we restrict consideration to the most natural initially thawing models, those with $1 + w_i < 5 \times 10^{-4}$ (recall most standard thawers have $1 + w_i \approx 10^{-4}$), then the percentages become 60%, 28%, 12% respectively. Thus there is no shortage of thawing models today.

### D. Monte Carlo Constraints

In the previous subsections we made use of a grid tessellation of parameter space to examine the variety of $w$-$w'$ phase space behaviors that can be obtained within the flow formalism. Here we will probe constraints on the $F(a)$ parameter space. In particular, we are interested in the ability to distinguish between model classes given observational data, and secondarily to determine the values of the flow parameters. We focus on the capability of future observations to rule out the cosmological constant,

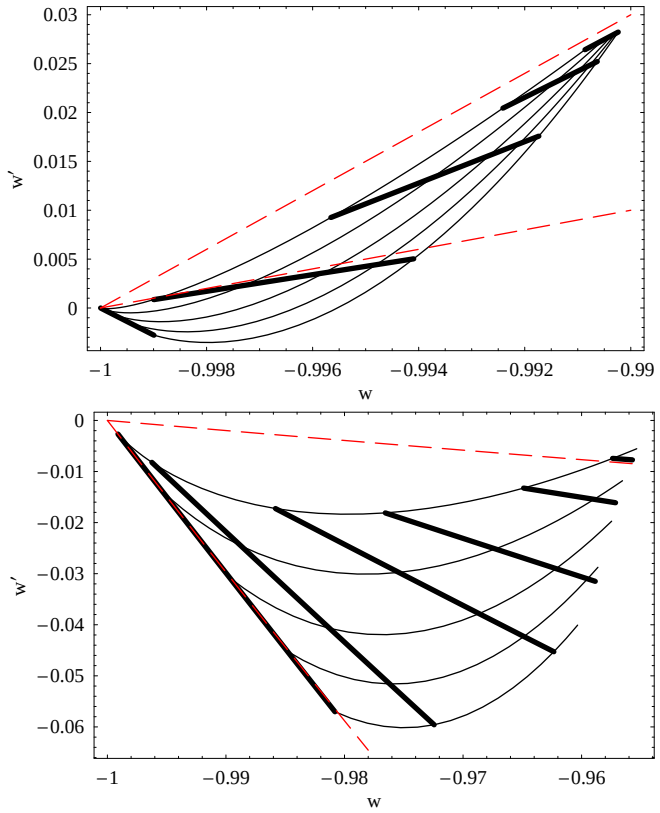


FIG. 10: For the present values of the equation of state parameters $w_0$ and $w_0'$, the influence of flow parameters $\beta$ and $B$ are illustrated. The isocontours of $\beta$ (thick lines) are shown for $\beta = 1$, 0.11, 0.033, 0.01, 0.0032 from bottom to top for the top panel ($\beta = 1$, 0.5, 0.2, 0.11, 0.05, 0.02 from left to right for the bottom panel). Isocontours of $B$ (thin lines) are shown for $B = 1$, 2, 3, 4, 5 from top to bottom. The top panel shows the initially thawing case, the bottom panel the initially freezing case, with the dashed lines showing the conventional boundaries for each region.

for example through measuring an evolution through a nonzero $\beta$ or finding the high redshift ($z \gtrsim 10$) equation of state value $w_i$ different from $-1$.

To quantify this, we generate data using a fiducial model and perform a Markov Chain Monte Carlo (MCMC) likelihood analysis [26–30] on the $F(a)$ parameters which, together with the initial value of the equation of state parameter $w_i$, fully determine the evolution of the dark energy. The usual ΛCDM model corresponds to $w_i = -1$ and the best fit is achieved with a set of parameters that select from the prior the smallest value of $1 + w_i$ (to start close to Λ), the largest of $\beta$ (to make the field quickly freeze, i.e. approach Λ), and the smallest value of $B$ (to start the freezing evolution early). Basically the cosmological constant behavior is an asymptotic state for scalar field dynamics. Because of this, the likelihood would concentrate around the prior bounds for whatever ranges we choose, making the predictions prior dependent. To avoid this, we instead choose a fiducial cosmology distinct from ΛCDM. This is of further interest since it explores the sensitivity of $F(a)$ parameters in revealing this deviation, should next generation datasets narrow in on a region of parameter space off ΛCDM.

Following the approach of the previous sections we study thawing and freezing models separately since these have well defined, high-redshift responses to the flow function $F(a)$. Accordingly, we select $F_0$ equal to 4/27 and 1/3, respectively. As discussed in Sec. III, fields with initial $F$ values different from these either betray matter domination, dilute very fast, or are finely tuned coasters. Nonetheless we emphasize that $F_0$ merely determines the high redshift initial conditions of the field and other parameters govern its late time dynamics. The distinction between thawing and freezing origin motivates further a different choice of priors for $1 + w_i$, since the different initial behavior of $w(a)$ is one of the features distinguishing between the two classes of models. For thawers, $1 + w_i$ is related to the initial energy density $\Omega_{\phi,i}$ and can be quite small, so we choose a logarithmic prior on $1 + w_i$ for the thawing models; for trackers, $1 + w_i$ tends to be larger so we choose a uniform prior on $1 + w_i$ for the (tracker) freezer case. Similarly, since $\beta$ tends to be larger in the freezing case we choose a uniform prior there but a logarithmic prior for the thawer case. The bounds on the priors, however, are the same as for the previous grid scanning: $1 + w_i \in [10^{-5}, 1]$, $\beta \in [10^{-5/2}, 1]$, and $B \in [1, 5]$.

The fiducial cosmology for both classes of models is chosen to be a maximum distance deviation of $\sim 1\%$ away from ΛCDM, to test the constraint capability of next generation observations. We assume data of 1% accuracy in distance at redshifts $z = 0.1, 0.2, \ldots 1.7$. This allows us to explore the degree to which the data can distinguish between the fiducial (thawing or freezing), its opposite class (freezing or thawing), and the cosmological constant. When considering a thawing fiducial we adopt $F_0 = 4/27$, $1 + w_i = 10^{-4}$, $\beta = 0.04$, and $B = 2$. For a freezing fiducial we take $F_0 = 1/3$, $w_i = -0.75$, $\beta = 0.6$, and $B = 1.5$.

The MCMC sampling of parameter space is done with the Metropolis-Hastings algorithm, using a Gaussian proposal distribution and fours chains per case. Computation of probability distributions and likelihood contours is done using a modified version of the GetDist package, provided with the CosmoMC software [28]. We define $w_i = w(a_i)$ with $a_i = 0.1$ and define the present by $\Omega_{\phi,0} = 0.72$. We integrate the coupled equations

$$w' = -3\,(1-w)^2\left[1-\frac{1}{\sqrt{3F}}\right] \quad (9)$$

$$\Omega_\phi' = -3w\Omega_\phi\,(1-\Omega_\phi) \quad (10)$$

$$d' = a^{-1}\sqrt{\frac{1-\Omega_\phi}{(1-\Omega_{\phi,0})\,a^{-3}}}\,, \quad (11)$$

where $d(a)$ is the conformal distance and a prime denotes $d/d\ln a$. The likelihood is based on the comparison of $d(a)$ for a $F(a)$ model to $d(a)$ for the fiducial.

The probability distributions for the thawing and freezing fiducial cases are shown in Fig. 11 (left and right panels respectively). We find $w_i$ to be the parameter best constrained, with clear distinct regions of excluded parameter space. In particular, the likelihood pulls away from the lower bound of the prior, preferring that $1 + w_i > 10^{-5}$ and thus demonstrating a distinction from the cosmological constant. The flow deviation amplitude $\beta$ is less well constrained, but for the thawing fiducial case the likelihood has some preference for smaller values, in contrast to the freezing class. For the freezing fiducial case, the contour prefers larger values of $\beta$, disfavoring a fit by thawing models. As mentioned previously, the evolution rapidity $B$ is essentially unconstrained. We emphasize that the flow approach is not intended as a new parametrization to fit specific models, but rather a useful tool for distinguishing classes of physics, in particular with respect to the high redshift behavior.

For both thawing and freezing fiducial cases the 2-dimensional joint probability distributions for $(w_i, \beta)$ and $(w_i, B)$ are each almost decorrelated. The exception is for large values of $\beta$ (large overall flow $F(a)$) where $w(a)$ need not start as negative since the evolution is pushed strongly toward ΛCDM. For $(w_i, B)$ the correlation is even weaker, and $w_i$ is insensitive to $B$ for most of its range except for very small values of $B$ (corresponding to an earlier flow deviation, evolving towards ΛCDM), where $w_i$ can be further away from the cosmological constant behavior. These results show that, while as expected a three parameter description of the equation of state cannot be tightly constrained, the key discriminating parameter of $w_i$ can be constrained. This allows distinction (for this 1% deviating fiducial at least) between each of the main classes of dark energy: a static cosmological constant, an initially thawing field, and an initially freezing field.

## V. COMPARING APPROACHES

Throughout most of this article we propounded the use of the flow quantity $F$ as a natural and slowly-evolving function, which could be relied upon to be approximately constant over a large number of $e$-folds. Unlike the case of parametrization of the scalar field potential, for which we need to assume some knowledge of its form and hence restriction to a particular case, the flow function $F(a)$ possesses natural characteristics that allow us some insight on the dynamics of the field, on the sole assumption of matter domination, without having to assume some explicit form for $V(\phi)$.

It is interesting to explore this argument further by showing that the opposite approach, a Taylor expansion of the potential as is often used (cf. [14, 17]), can lead to results which don't fully or faithfully describe the available and viable dynamics. Indeed its consistency as a description of the potential can break down, as the quantities in which it is being expanded are not generally small. Such is the case of the (not necessarily slowly rolling) slow-roll parameters $\epsilon(\phi)$ and $\eta(\phi)$, defined in terms of first and second derivatives of the potential, or the field displacement $\Delta\phi$.

The usual parametrization of the potential based on the slow-roll assumption takes

$$V(\phi)/V(\phi_0 = 0) \sim 1 + V_1\phi + V_2\phi^2 + ... \qquad (12)$$

where $\phi_0$ (taken to be zero without loss of generality) is the field value at some initial scale factor $a_i$, $V_0$ is the initial value of the potential energy density, and the coefficients of the expansion are expressed in terms of the usual slow-roll parameters [31–36] with $V_1 = -\sqrt{16\pi\epsilon_i}$, and $V_2 = 4\pi\eta_i$.

For the validity of Eq. (12) as a Taylor expansion, one needs either to rely on a sufficiently flat potential, by having small slow-roll parameters initially, or to take the expansion to be valid over a narrow region of the field trajectory, such that for the range of potential we are interested in (i.e. its evolution up to the present) $\Delta\phi$ is small. In particular, we would want $\Delta\phi \ll (16\pi\epsilon)^{-1/2}$ and $\Delta\phi \ll (\epsilon/[\pi\eta^2])^{1/2}$ to have convergence, i.e. the linear being smaller than the constant term, and the quadratic term smaller than the linear term, respectively.

However, remember there is no guarantee the potential is sufficiently flat, today or at high redshift. This in turn gives no grounds for taking small bounds on the slow-roll parameters, in Monte Carlo simulations or other analyses. Indeed the detailed analysis of [17] finds values of $\epsilon_i \approx 1$ and $\eta_i \approx 5$, or greater, to be within the 68% confidence limits contour at $z_i = 3$ (for current distance data taken from supernovae, baryon acoustic oscillation, cosmic microwave background, and Hubble constant measurements; note they use the potential as a quadratic or cubic form, not a Taylor expansion per se). If instead one tries to ensure validity of a (truly) slow-roll expansion by artificially imposing small $\epsilon_i$ (or equivalently starting the field at rest), one obtains strongly restricted dynamics as seen in the clear analysis and Fig. 9 of [17], which shows much narrower $w(a)$ evolutions than in the absence of this imposition.

To highlight the influence of matter domination on the slow-roll parameters in the potential model, we tested starting the initial conditions at different redshifts and following the evolution of $\epsilon$ and $\eta$. If instead of imposing $\epsilon_i = 1$, $\eta_i = 5$ at $z_i = 3$, we start with these values at higher redshift, $z_i = 9$, then by $z = 3$ the first slow-roll quantity has dropped to $\epsilon \approx 0.01$ ($\eta$ stays fairly constant), clearly demonstrating the governing influence of matter domination.

This reduction is insensitive to the initial redshift – as long as it is at least one $e$-fold before the evaluation point at $z = 3$. Thus, if one wants to carry out Monte Carlo simulations, either one can use a wide range for the parameters – but the initial conditions should be set at least a few $e$-folds into matter domination, or for a more

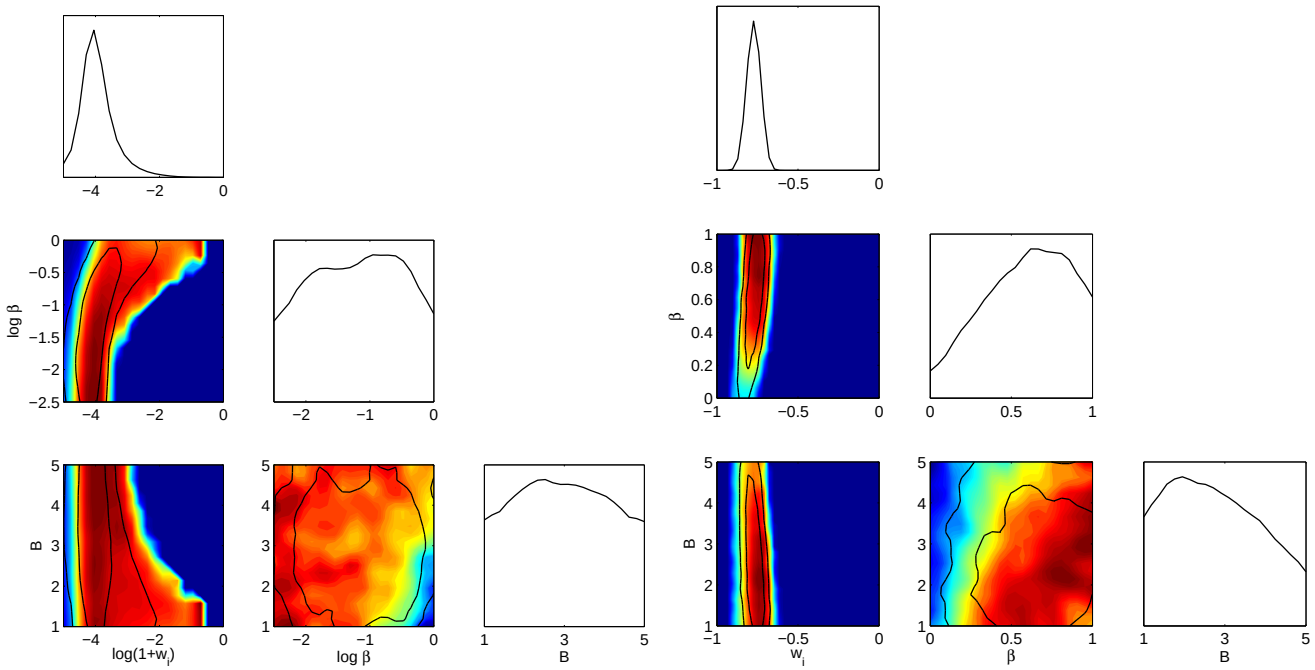


FIG. 11: 1- and 2-dimensional marginalized probability distributions and contours of MCMC reconstruction of the flow parameters are illustrated for next generation distance data. The left panel shows results for the thawing case, with $F_0 = 4/27$, which used log priors on $1 + w_i$ and $\beta$; the right panel shows the distributions for the tracker/freezing case, with $F_0 = 1/3$, which used uniform priors to take into account the larger fiducial values. The diagonal panels correspond to the marginalized 1D probability distributions and the off diagonal to the marginalized 2D joint distributions. Thick curves in the off diagonal plots show the 68% and 95% likelihood contours and the color grading denotes the marginalized probability density from (red) highest to (blue) lowest. The MCMC constraints clearly recognize small $1 + w_i$ for thawing, distinct from the large values typical of freezing models and from the zero value of the cosmological constant. For freezing, again $w_i$ is distinct from the cosmological constant and from typical thawing values. The parameter $\beta$ shows tendencies toward the expected preference for small values for thawing and larger values for freezing, but the constraints are not tight. Most importantly, the thawing and freezing classes can be distinguished from each other and from the cosmological constant.

recent start one should use a restricted range of initial conditions as given by the matter dominated physics.

In addition, in order to apply the Taylor expanded potential formalism one needs to rely on a small field excursion during the relevant dark energy evolution. In terms of the slow-roll parameters, for $\epsilon \approx 1$, $\eta \approx 5$ the convergence conditions mentioned above require $\Delta\phi \ll 0.14$ and $\Delta\phi \ll 0.11$. With the aim of testing this assumption we compute the field displacement $\Delta\phi$ incurred for the flow models we considered previously, between the initial redshift and today, conservatively selecting those which most resemble ΛCDM, since $\Delta\phi$ is smallest for these. We will find that we cannot guarantee the necessary level of smallness to validate the potential approximation.

From the expression for the scalar field kinetic energy (see above Eq. 2), the effective field excursion $\Delta\phi$ between the initial redshift, $z_i = 9$ and today is

$$\Delta\phi = \int_{a_i}^{1} \frac{da}{a} \sqrt{3\Omega_\phi\,(1+w)}\,. \qquad (13)$$

We compute $\Delta\phi$ for the flow models from Sec. IV that pass the 1% distance criteria. For thawing models the main contribution to $\Delta\phi$ is during the last $e$-fold or so, and accordingly we find a relatively small field displacement for thawers, of $\Delta\phi \approx 0.06$ for $w_i = -1 + 10^{-5}$ and up to $\Delta\phi \approx 0.4$ for the top of the range $w_i = -0.99$.

On the other hand for the freezing behavior there is the possibility of a more substantial contribution to the field excursion throughout the evolution since the dark energy density is larger at early times and the equation of state finds its way towards Λ from larger $w_i$. For freezers we obtain $0.014 < \Delta\phi < 0.53$ between the smallest to the largest $w_i$, $-0.99 < w_i < -0.36$.

Both for thawers and freezers the leading influence on $\Delta\phi$ among the flow parameters is $w_i$. For thawers this is straightforward since $w(a)$ increases constantly with $w_i$ – apart from those models which cross $F = 1/3$ and turn around, receding back toward ΛCDM: for those $\Delta\phi$ will be smaller than in the purely thawing case.

The freezing dark energy case is different: large $w_i$ will cause the field to travel longer initially, before it slows down towards $w \approx -1$ in order to meet the distance criteria. For these fields particularly, it is crucial to initialize the evolution equations at high enough redshift, where the field is evolving the most and determining the conditions for its later dynamics. Starting the evolution

at $z = 3$, only 1.4 $e$-folds before the present, is problematic and can change the results. For example, using $z_i = 3$ Ref. [17] finds an average of $\Delta\phi = 0.09 \pm 0.03$, out of their posterior distribution obtained from current data, 74% of the models being freezer models. Our results using $z_i = 9$ for the flow model give significantly different results; even for models that closely resemble $\Lambda$ we find values as large as $\Delta\phi = 0.34$ between $z = 3$ and $z = 0$, for freezer models. Interestingly, in the absence of the slow-roll assumption either in the form of small slope or small field displacement, one finds the allowed field dynamics to be both richer and simultaneously able to remain close to $\Lambda$CDM.

This argument becomes all the more important if we remember we don't have any guarantee today of distance measurements agreeing with $\Lambda$CDM to 1%. Relaxing this would further release the behavior of freezer models early on, and can give large field excursions, for example $\Delta\phi = 0.87$ for an $n = 1$ SUGRA model [37], with a maximum 3% distance deviation for $z < 1.7$.

Thus the flow parameter approach appears to have a certain amount of natural motivation, from the long era of matter domination, and can offer a self-consistent approach. It is also important to note that the appropriate initial conditions must be carefully considered for a Monte Carlo analysis of the field evolution.

Because the relation $w'(w)$ can be written either in terms of the flow $F$ or the potential parameters, e.g. $\lambda \equiv -(1/V)dV/d\phi$ and $\Omega_\phi$, interchangeably through $F = (1 + w)/[\Omega_\phi \lambda^2]$, the near constancy of $F$ implies that one cannot arbitrarily choose $\lambda$, $\Omega_\phi$, and $w_i$ in the Monte Carlo initial conditions during matter domination. Moreover, if any of $1 + w$, $\Omega_\phi$, or $\lambda^2$ start too large (including taking a uniform prior out to a relatively large upper bound), then generating realizations of the thawing class of models will be strongly suppressed. As mentioned previously, even a large initial value of $\epsilon$ ($\sim \lambda^2$), if the evolution takes into account matter domination, becomes a much more restricted value by $z = 3$ (this accords with Figure 9 of [17] where once they restrict the initial value of $\epsilon$, a substantial fraction of randomly generated models become otherwise scarce thawers). While the flow approach is not without flaw, it does present an interesting alternative, one that innately incorporates the role of the long matter dominated era and the oldness of dark energy.

## VI. CONCLUSIONS

Dark energy does not exist in a vacuum. For dozens of $e$-folds of Hubble expansion it was dominated by matter and radiation, and has risen above them for only a fraction of the last $e$-fold. This has a definite effect on the dynamical evolution of dark energy, aging or mellowing it. In particular, a wide range of models exhibit a nearly constant flow parameter, relating the deviation of the equation of state from $-1$, the deviation of the dark energy density from 0, and the slope of the potential. It is not until $z \gtrsim 2$ that the flow parameter, and the equivalent relation between $w'$ and $w$, is generally free to vary.

This characteristic suggests the flow parameter is an interesting quantity to use for parametrizing the dark energy evolution, one that can intrinsically take into account the oldness of dark energy. We have examined an evolutionary model for the deviations of the flow parameter from constancy as matter domination wanes and acceleration occurs. This gives rise to a variety of dynamical behaviors in the $w'$-$w$ phase space, incorporating thawing, freezing, and "refreezing" classes. Observational constraints on the dark energy equation of state, e.g. through distance-redshift measurements, bound specific regions in the $w'$-$w$ plane. For example, scanning 250,000 models, we illustrate the region, and its component classes, of maximum deviation allowed away from $w = -1$. We also identify an interesting "waist" phenomenon – independent of the standard $w_0$-$w_a$ parametrization – where at a certain redshift the equation of state is tightly constrained.

With an MCMC analysis one can quantify the bounds on the values of the flow parameters allowed by distance measurements. In particular this permits determination of the high redshift dark energy equation of state, a key parameter for the important physics question of distinguishing between a cosmological constant, initially thawing models, and initially freezing models. Finally, we emphasize that taking into account the maturity of dark energy is important for MCMC generation of models since random initial conditions, e.g. on the potential, do not appropriately sample the "diversity under constraint" of old dark energy.

### Acknowledgments

We thank Sarah Bridle, Dragan Huterer, Andrew Liddle, Hiranya Peiris, and Anže Slosar for discussions, and are especially grateful to Martin Kunz and David Parkinson for helpful advice. MC thanks the Institute for the Early Universe at Ewha University, IPMU in Japan, and Shinji Tsujikawa and the Tokyo University of Science, for hospitality. We acknowledge the use of the computer system at the Astronomy Centre at the University of Sussex. This work has been supported in part by the Director, Office of Science, Office of High Energy Physics, of the U.S. Department of Energy under Contract No. DE-AC02-05CH11231.

[1] E.V. Linder, Phys. Rev. D 73, 063010 (2006) [arXiv:astro-ph/0601052]

[2] R.N. Cahn, R. de Putter, E.V. Linder, JCAP 0811, 015

(2008) [arXiv:0807.1346]
[3] R.R. Caldwell & E.V. Linder, Phys. Rev. Lett. 95, 141301 (2005) [arXiv:astro-ph/0505494]
[4] B. Ratra & P.J.E. Peebles, Phys. Rev. D 37, 3406 (1988)
[5] C. Wetterich, Nucl. Phys. B 302, 668 (1988)
[6] J.A. Frieman, C.T. Hill, A. Stebbins, I. Waga, Phys. Rev. Lett. 75, 2077 (1995) [arXiv:astro-ph/9505060]
[7] P.G. Ferreira & M. Joyce, M., Phys. Rev. Lett. 79, 4740 (1997) [arXiv:astro-ph/9707286]
[8] I. Zlatev, L. Wang, P.J. Steinhardt, Phys. Rev. Lett. 82, 896 (1999) [arXiv:astro-ph/9807002]
[9] A.R. Liddle & R.J. Scherrer, Phys. Rev. D 59, 023509 (1999) [arXiv:astro-ph/9809272]
[10] P.J. Steinhardt, L. Wang, I. Zlatev, Phys. Rev. D 59, 123504 (1999) [arXiv:astro-ph/9812313]
[11] R.J. Scherrer & A.A. Sen, Phys. Rev. D 77, 083515 (2008) [arXiv:0712.3450]
[12] D. Huterer & M.S. Turner, Phys. Rev. D 60, 081301 (1999) [arXiv:astro-ph/9808133]
[13] J. Simon, L. Verde, R. Jimenez, Phys. Rev. D 71, 123001 (2005) [arXiv:astro-ph/0412269]
[14] M. Sahlén, A.R. Liddle, D. Parkinson, Phys. Rev. D 72, 083511 (2005) [arXiv:astro-ph/0506696]
[15] M. Sahlén, A.R. Liddle, D. Parkinson, Phys. Rev. D 75, 023502 (2007) [arXiv:astro-ph/0610812]
[16] T.G. Clemson, A.R. Liddle, MNRAS 395, 1585 (2009) [arXiv:0811.4676]
[17] D. Huterer & H.V. Peiris, Phys. Rev. D 75, 083503 (2007) [arXiv:astro-ph/0610427]
[18] R. Crittenden, E. Majerotto, F. Piazza, Phys. Rev. Lett. 98, 251301 (2007) [arXiv:astro-ph/0702003]
[19] E.V. Linder, Astropart. Phys. 24, 391 (2005) [arXiv:astro-ph/0508333]
[20] M. Doran, G. Robbers, C. Wetterich, Phys. Rev. D 75, 023003 (2007) [arXiv:astro-ph/0609814]
[21] E.V. Linder & D. Huterer, Phys. Rev. D 72, 043509 (2005) [arXiv:astro-ph/0505330]
[22] R. de Putter & E.V. Linder, Astropart. Phys. 29, 424 (2008) [arXiv:0710.0373]
[23] D. Rapetti, S.W. Allen, J. Weller, MNRAS 360, 555 (2005) [arXiv:astro-ph/0409574]
[24] E.V. Linder, Gen. Rel. Grav. 40, 329 (2008) [arXiv:0704.2064]
[25] E.V. Linder, arXiv:0708.0024
[26] D. J. C. MacKay, Information theory, inference and learning algorithms, Cambridge University Press (2003)
[27] W. R. Gilks, S. Richardson, D. J. Spiegelhalter (eds.), Markov Chain Monte Carlo in Practice, Chapman & Hall (1996)
[28] A. Lewis and S. Bridle, Phys. Rev. D 66, 103511 (2002) [arXiv:astro-ph/0205436]
[29] J. Dunkley, M. Bucher, P. G. Ferreira, K. Moodley, C. Skordis, MNRAS 356, 925 (2005) [arXiv:astro-ph/0405462]
[30] A.R. Liddle, Annual Review of Nuclear and Particle Science 59 (2009) [arXiv:0903.4210]
[31] A. R. Liddle, P. Parsons, J.D. Barrow, Phys. Rev. D50, 7222 (1994) [arXiv:astro-ph/9408015]
[32] M.B. Hoffman, M.S.Turner, Phys. Rev. D64, 023506 (2001) [arXiv:astro-ph/0006321]
[33] W.H. Kinney, Phys. Rev. D66, 083508 (2002) [arXiv:astro-ph/0206032]
[34] R. Easther, W.H. Kinney, Phys. Rev. D67, 043511 (2003) [arXiv:astro-ph/0210345]
[35] A.R. Liddle, Phys. Rev. D68, 103504 (2003) [arXiv:astro-ph/0307286]
[36] H. Peiris, R.Easther, JCAP 0610, 017 (2006) [arXiv:astro-ph/0609003]
[37] P. Brax & J. Martin, Phys. Lett. B 468, 40 (1999) [arXiv:astro-ph/9905040]